Hindawi
Journal of Nanomaterials
Volume 2022, Article ID 6237698, 11 pages
https://doi.org/10.1155/2022/6237698

Research Article

Nonlinear Convective SiO_2 and TiO_2 Hybrid Nanofluid Flow over an Inclined Stretched Surface

Sehrish,[1] Said Anwar Shah,[2] Abir Mouldi,[3] and Ndolane Sene[4]

[1]*Department of Mathematics and Statistics, Bacha Khan University, Charsadda, Pakistan*
[2]*Department of Basic Sciences & Islamiat, University of Engineering and Technology, Peshawar, Pakistan*
[3]*Department of Industrial Engineering, College of Engineering, King Khalid University, Abha 61421, Saudi Arabia*
[4]*Laboratoire Lmdan, Departement de Mathematiques de Decision, Facultíe des Sciences Economiques et Gestion, Universite Cheikh Anta Diop de Dakar, BP 5683 Dakar Fann, Senegal*

Correspondence should be addressed to Ndolane Sene; ndolanesene@yahoo.fr

Received 8 January 2022; Accepted 15 March 2022; Published 4 May 2022

Academic Editor: Amir Khan

The hybrid nanofluid is extensively used in manufacturing commercial applications due to its high exceptional capacity to increase the heat transfer rate. As a result, in the existence of nonlinear convection, the hybrid nanofluid is considered to flow on an inclined plane. The nonlinear convection has many applications in real life and is more relevant to the natural flow avoiding the flow restrictions. The focus has been executed on the thermal and mass Grashof numbers to analyse the fluid motion in the presence of these parameters for nonlinear nature. Moreover, the hybrid nanofluid flow analysis has been done to investigate the heat transfer analysis. The modelled equations are solved through an analytical approach. The heat and mass transfer rates and drag force are calculated under the influence of various physical parameters. The new parameter of the Grashof numbers improves the fluid motion for its larger values, and consequently, the fluid rapidly falls down from the inclined plane. The obtained outputs show that hybrid nanofluids are more effective in heat transfer analysis as compared to other conventional fluids.

1. Introduction

In the past few years, the utilization of thin-film liquid flow has fascinated researchers in the different area like engineering, technology, and industry; consequently, the study of thin-film liquid flow analysis regarding their application in many fields is necessary such as shipment through the flow in human lung and a lubricating process in the industry. These and a few more are considered to be the biggest subclass of thin-film liquid flow-related issues. The study of thin-film liquid flow in many active applications is a nice combination of structural mechanics, fluid mechanics, and theology. One of its main applications is the cable fiber undercoat. In addition, polymer and metal extrusion, food straightening, permanent formulation, elastic sheet drawing, and device fluidization, exchange, and chemical treatment apparatus are some of the well-known uses. Observing these applications, it became the principal subject for the investigator to study and analyse the behaviour of thin-film liquid flow at stretching surfaces. The flow behaviour for the first time regarding thin-film was investigated through Newtonian liquids and then expanded to non-Newtonian liquids. The non-Newtonian thin-film flow of nanoliquids has been analysed by Sandeep et al. [1]. Wang [2] has examined the transient thin-film liquid flow at the stretching surface. The motion of thin-film finite fluid at the time-dependent stretching surface was analysed by Usha et al. [3]. Liu et al. [4] have studied the movement of thin-film liquid regarding heat transfer behaviours at a stretching surface. Aziz et al. [5] examined thermal generation within thin-film liquid flow at a stretching sheet. The thin-film liquid motion with heat radiation regarding the behaviour of heat transmission has been analysed by Tawade et al. [6]. They solved their proposed model using Runge-Kutta-Fehlberg and Newton method. The analysis of heat transfer through thin-film liquid flow at a stretching surface has been done by Anderssona et al. [7]. Many researchers have worked independently on power-law liquid motion using thin-film time-dependent stretching sheets [8–11]. Megahe [12] has studied the flow of thin film of Casson liquid with heat transfer on a transient stretching sheet. In the proposed model, they also considered the slip velocity impact with heat flux and viscous dissipation. In the recent past, Tahir et al. [13] and Khan et al. [14] analysed the motion of thin-film nanoliquid through innovative approach. The growing interest in energy reserves is one of the most complicated issues for current researchers to fulfill the augmenting requirements for energy in modern scientific practices. Researchers are attempting to introduce new channel of energy that are convenient and reasonable for cooling and thermal applications. The most readily approachable means of renewable energy in the universe is solar energy. Solar energy is a good source of clean and renewable energy, so it will not cause environmental adulteration which is generated by conventional energy such as coal, oil during the process of use. The negative impacts of pollution on the earth cause global warming and lung and cancer disease. Solar energy is a good alternative to surmount this problem and reduce its detrimental impacts. Over the past 30 years, many developed and developing industrialized countries have focused on advancing solar technology. When there is oil, energy crisis, solar energy becomes more attractive. The oil crisis in general is a crisis of higher prices as OPEC countries raise fuel prices, so options include solar thermal, solar photovoltaic, wind energy, geothermal, marine, and wave energy. So scientists and researchers paid attention to all these things, and an interesting reality is that the energy that approaches the earth from 20 days of sunlight is equal to the energy stored in all the earth's storages of fossil fuels such as petroleum, coal, and natural gas. In this way, they play a prominent role in meeting the needs of the people in the world. Flat plates (solar collectors) use heat transfer liquids to transform solar energy into thermal energy. Rising energy needs around the world, including nonrenewable energy sources like fossil fuels, have minimal production of such resources, resulting in huge, detrimental effects on the environment, like global warming, climate change, and air pollution. To mitigate such losses, scientific approach has focused on improving the productivity of renewable energy processes, like solar energy. Solar energy is the cheapest and cleanest option of renewable energy, which converts solar energy into environmentally friendly electrical and thermal energy. For the conversion of solar energy into heat energy, a heat-changing liquid can be used in flat plate-type solar collectors [15]. Solar collectors receive solar rays through absorbing plates and converting such rays into a useful form of the energy (primarily water, water composition, and EG). Nevertheless, the major shortcomings are the low thermal properties of these conventional liquids, as they offer low thermal efficiency in the transformation process. Converting conventional working liquids into nanoliquids is one of the initiatives, which has received more attention over the past few years in enhancing the thermal efficiency of this technology. A stable synthesis of solids components between 1 nm and 100 nm is referred to nanoliquids [16]. Nanoliquid is also widely utilized in solar energy depots [17, 18], heat exchangers [19], and freezing methods [20]. Mebarek-Oudina [21] studied nanofluid using various basic fluids. An analytical study of MHD nanoliquid motion, for heat transfer analysis, was done by Saeed and Gul [22]. Rehman et al. [23] analysed the motion of nanofluids by implementing the induced changeable magnetic field using the liquid film flow model. The motion of Darcy–Forchheimer nanoliquid through a mathematical model at the curved surfaces was analysed by Sajjad et al. [24]. Several recent analyses have been done in different energy and thermal environments using analytical and numerical methods, for handling heat exchanges and nanoliquid flow behaviour, by Sheikholeslami [25], Zhang et al. [26], and Gul et al. [27]. The magnetic properties of an electrically conducting liquid are referred to as MHD. In the natural and industrial spheres, we can notice that the behaviour of liquid motion is influenced by magnetic fields. The MHD phenomenon occurs when the velocity and magnetic field are combined. Instances of these kinds of fluids are liquid metals, electrolytes, plasma, etc. The concept of magnetohydrodynamic has been invented by Hannes Alfven [28]. On this great success, he was given the Nobel Prize in Physics in 1970. MHD has many applications in engineering and technologies such as MHD generators, plasma, and nuclear reactors. The use of solar energy collectors also plays a significant role in medicine such as cancer therapy and MRI. This study is about the movements of ionized atoms or components and their liaison with the electric fields and neighbouring liquids. This safeguards against particle (atoms or molecules) and fluid transport phenomena such as electrorotation, dielectrophoresis, electro-osmosis, and electrokinesis. This has wide range of applications in many areas including gas pumps, drag reduction, increasing drying rate, and plasma actuators. At the outset, electrohydrodynamic fluid motion has been examined by Woodson and Melcher [29]. The impact of substitutive current and thermal transport on the dielectric viscous peristaltic fluid motion has been examined by Sayed et al. [30]. Khan et al. [31] investigated the irreversible behaviour of the electromagnetic hydrodynamic convective flow of viscous fluid. Rashid et al. [32] scrutinized the micro polar electromagnetohydrodynamic radiative fluid flow with convection state at a stretchable permeable sheet. In the recent past, scientists have focused on the fluids flowing at the permeable space and particles of various shapes inside the porous region. Their use can be understood in the multiple fields like nuclear engineering, environmental sciences, solar thermal engineering, bioinformatics, and construction engineering. Several processes that require the movement of fluids in a porous region include the utilization of geothermal energy, the flow of blood to lungs or veins, below-ground power lines, porous heating pipes, and chemically catalytic combiners. To understand the movements of fluid in porous space, Darcy's law is used frequently. Darcy's notion of high velocity and turbulent impacts in the porous space is wrong. Mebarek-Oudina et al. [21, 33–35] investigated the MHD hybrid nanofluid flow through various configuration and geometries in the presence of different nanomaterials.

Forchheimer [36] updated the momentum expression through the inclusion of second-order polynomial to adjust the impact of inertia on relative permeability. To analyse the impacts of inertia at relative permeability, a term of second-order polynomial in the momentum equation has been introduced by Forchheimer [36]. Muskat [37] pointed out that component as a Forchheimer component. Many researchers have investigated the fluid motion via porous media by utilizing the Darcy–Forchheimer idea in various geometries. Few of them are presented here. Saif et al. [24] explained the motion of nanoliquid in the porous gap and concluded that the fluctuation in the fluid flow forms the surface of the stretchable curve. The behaviour of nanofluid motion regarding Darcy–Forchheimer effects produced through a stretching sheet, as explored by Rasool et al. [38]. A Darcy–Forchheimer flow of liquid at a spinning disc has been explored by Sadiq et al. [39]. A non-Darcy liquid flow within a transparent gap is explained by Sheikholeslami et al. [40]. The impacts of Darcy–Forchheimer and EMHD on the movement of viscous liquid in the presence of Joule heating and heat flux at a stretching surface were scrutinized by Hayat et al. [41, 42]. In addition, they studied the process of entropy generation with the aid of the second law of thermodynamics. Kumar et al. [43] calculated the numerical outcomes of CNT nanofluids movement by the numerical scheme in divergent and convergent channels under the effects of thermal radiation. Akgül et al. [44–49] presented different novel technique for investigating fractional differential equations including the Atangana-Baleanu fractional derivative. The relevant and latest literature can be seen as [50–52].

The main objective of the ongoing research is to analyse the impact of electro-hydrodynamic Darcy–Forchheimer liquid movement and its use in augmenting the capacity of solar collectors through inclined plates. The energy equation has been developed under Joule heating, heat radiation, and viscous dissipation. The proposed model of the fluid flow has been formulated through PDEs and subsequently solved analytically in Mathematica using HAM technique. The analysis of different significant emerging parameters is elucidated in terms of temperature, velocity, and concentration. The numerical findings of the proposed model have been validated through findings in the literature. It reveals that the outcomes of the model are real and applicable in many fields of engineering and science.

The newness of the proposed model is as follows.

(I) The inclined plane with nonlinear mixed convection is used for the first time

(II) The nanoparticles TiO_2 and SiO_2 are used

(III) The skin friction and Nusselt numbers are displayed through charts for the impact of different parameters

(IV) HAM method has been used for the solution

2. Mathematical Formulation

A 2D steady fluid motion at a stretchable inclined plate is studied, which makes θ angle along with vertical axis, as shown in Figure 1, as a solar collector schematic outlook. The space is presumed as a porous Darcy–Forchheimer. In addition, the energy equation is updated through the inclusion of heat radiation, viscous dissipation, and Joule heating.

The term $\vec{J} \times \vec{B}$ is referred to as Lorentz force, where $\vec{B}$ and $\vec{J}$ are the magnetic field and current density, respectively. Ohm's law can be stated as $\vec{J} = \sigma(\vec{E} + \vec{V} \times \vec{B})$, E stands for electric field, and it is presumed that $\vec{E} = 0$. In addition, T_w, T_∞, C_w, and C_∞ are wall's temperature, free-stream temperature, wall's concentration, and free-stream concentration, respectively. Using the above principles, the mathematical formulation of the proposed model is [21, 22, 25, 53]

$$\frac{\partial u}{\partial x} + \frac{\partial v}{\partial y} = 0, \tag{1}$$

$$\begin{aligned}\rho_{\mathrm{hnf}}\left(u\frac{\partial u}{\partial x} + v\frac{\partial u}{\partial y}\right) &= \mu_{\mathrm{hnf}}\left(\frac{\partial^2 u}{\partial y^2}\right)\\ &\pm g\cos\theta\left[(T - T_\infty)(\rho\beta_T)_{\mathrm{hnf}} + (T - T_\infty)^2(\rho\beta_T)^2_{\mathrm{hnf}}\right.\\ &\left.+ (C - C_\infty)(\rho\beta_C)_{\mathrm{hnf}} + (C - C_\infty)^2(\rho\beta_C)^2_{\mathrm{hnf}}\right],\end{aligned} \tag{2}$$

$$\left(\rho c_p\right)_{\mathrm{hnf}}\left(u\frac{\partial T}{\partial x} + v\frac{\partial T}{\partial y}\right) = k_{\mathrm{hnf}}\frac{\partial T^2}{\partial y^2}, \tag{3}$$

$$\left(u\frac{\partial C}{\partial x} + v\frac{\partial C}{\partial y}\right) = D_{\mathrm{hnf}}\frac{\partial C^2}{\partial y^2}. \tag{4}$$

Acceptable boundary conditions are

$$u = bx = u_w(x), v = 0, C = C_w, T = T_w, \mathrm{at} y = 0, \tag{5}$$

$$u = 0 = v, C \longrightarrow C_\infty, T \longrightarrow T_\infty, \mathrm{at}\, y \longrightarrow \infty, \tag{6}$$

where K represents the porous medium permeability and u and v denote the velocity components in the x and y direction.

Using the following pertinent transformation variables,

$$u = F'(\eta)bx, v = -\sqrt{bv_f}F(\eta), (T_w - T_\infty)\Theta(\eta) = T - T_\infty, \tag{7}$$

$$(C_w - C_\infty)\Phi(\eta) = C - C_\infty, \eta = y\sqrt{\frac{b}{v_f}}. \tag{8}$$

The reduced form of Equations (1),(2),(3),(4),(5) in the

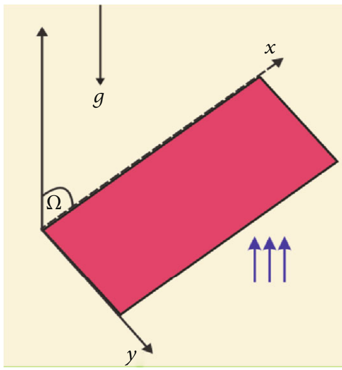

FIGURE 1: Geometry of the problem.

light of Equation (7) is as follows:

$$F''' + \frac{\rho_{hnf}}{\rho_f}\frac{\mu_f}{\mu_{hnf}}\left[FF'' - F'^2\right] + \frac{\mu_f}{\mu_{hnf}}\cos\theta\left[\begin{array}{c}\left[\frac{(\rho\beta_T)_{hnf}}{(\rho\beta_T)_f}Gr\Theta + \left(\frac{(\rho\beta_T)_{hnf}}{(\rho\beta_T)_f}\right)^2 Gr^*\Theta^2\right] \\ \pm\left[\frac{(\rho\beta_C)_{hnf}}{(\rho\beta_C)_f}Gc\Phi + \left(\frac{(\rho\beta_C)_{hnf}}{(\rho\beta_C)_f}\right)^2 Gc^*\Phi^2\right]\end{array}\right] = 0, \tag{9}$$

$$\frac{k_{hnf}}{k_f}\Theta'' + \Pr\frac{(\rho Cp)_{hnf}}{(\rho Cp)_f}F\Theta' = 0, \tag{10}$$

$$\frac{\mu_f}{\mu_{hnf}}\Phi'' + \mathrm{Sc}F\Phi' = 0. \tag{11}$$

With interrelated boundary conditions,

$$\mathrm{Gr} = \frac{g\beta_{Tf}(T_w - T_\infty)}{bu_w}, \tag{12}$$

$$\mathrm{Gr}^* = \frac{g\beta_{Tf}^2(T_w - T_\infty)^2}{bu_w}, \tag{13}$$

$$\mathrm{Gc} = \frac{g\beta_{Cf}(C_w - C_\infty)}{bu_w}, \tag{14}$$

$$\mathrm{Gc}^* = \frac{g\beta_{Cf}^2(C_w - C_\infty)^2}{bu_w}, \tag{15}$$

$$\Pr = \frac{\nu_f}{\alpha_f}, \tag{16}$$

$$\mathrm{Sc} = \frac{\upsilon_f}{D_B}. \tag{17}$$

The above physical quantities are Grashof number, Prandtl number, heat source/sink factor, and Schmidt number.

$$\nu_{hnf} = \frac{\mu_{hnf}}{\rho_{hnf}}, \tag{18}$$

$$\mu_{hnf} = \frac{\mu_f}{\left(1-\phi_{SiO_2}\right)^{5/2}\left(1-\phi_{TiO_2}\right)^{5/2}}, \tag{19}$$

$$\rho_{hnf} = \left(1-\phi_{TiO_2}\right)\left\{1-\left(1-\frac{\rho_{TiO_2}}{\rho_f}\right)\phi_{SiO_2}\right\} + \frac{\rho_{Ag}}{\rho_f}\phi_{TiO_2}, \tag{20}$$

$$(g\beta_T)_{hnf} = \left(1-\phi_{TiO_2}\right)\left\{1-\left(1-\frac{(\rho\beta_T)_{SiO_2}}{(\rho\beta_T)_f}\right)\phi_{SiO_2}\right\} + \frac{(\rho\beta_T)_{TiO_2}}{(\rho\beta_T)_f}\phi_{TiO_2}, \tag{21}$$

$$(g\beta_c)_{hnf} = \left(1-\phi_{TiO_2}\right)\left\{1-\left(1-\frac{(\rho\beta_c)_{SiO_2}}{(\rho\beta_c)_f}\right)\phi_{SiO_2}\right\} + \frac{(\rho\beta_c)_{TiO_2}}{(\rho\beta_c)_f}\phi_{TiO_2}, \tag{22}$$

$$\frac{(\rho C_p)_{hnf}}{(\rho C_p)_f} = \left(1-\phi_{TiO_2}\right)\left\{1-\left(1-\frac{(\rho C_p)_{SiO_2}}{(\rho C_p)_f}\right)\phi_{SiO_2}\right\} + \frac{(\rho C_p)_{TiO_2}}{(\rho C_p)_f}\phi_{TiO_2}, \tag{23}$$

$$\frac{k_{hnf}}{k_{nf}} = \left(\frac{k_{TiO_2} + 2k_{nf} - 2\phi_{TiO_2}\left(k_{nf} - k_{TiO_2}\right)}{k_{TiO_2} + 2k_{nf} + \phi_{TiO_2}\left(k_{nf} - k_{TiO_2}\right)}\right), \frac{k_{nf}}{k_f} = \left(\frac{k_{SiO_2} + 2k_f - 2\phi_{SiO_2}\left(k_f - k_{SiO_2}\right)}{k_{SiO_2} + 2k_f + \phi_{SiO_2}\left(k_f - k_{SiO_2}\right)}\right). \tag{24}$$

Furthermore, the additional most key physical number are skin friction coefficient (C_{fx}), Nusselt number (Nu_x), and Sherwood number written as

$$C_{fx} = \frac{\tau_w}{(1/2)\rho(u_w)^2}, \quad \mathrm{Nu}_x = \frac{xq_w}{k(T_w - T_\infty)}, \quad \mathrm{Sh}_x = \frac{xj_w}{D_B(T_w - T_\infty)}, \tag{25}$$

where τ_w is the shear stress and q_w denotes heat flux near the surface. Utilizing Equation (7), Equation (18) yields

$$C_{fx}\mathrm{Re}_x{}^{0.5} = 2\frac{\mu_{\mathrm{hnf}}}{\mu_f}F''(0),$$
$$\mathrm{Nu}_x\mathrm{Re}_x{}^{-0.5} = -\frac{k_{\mathrm{hnf}}}{k_f}\Theta'(0), \tag{26}$$
$$\mathrm{Sh}_x\mathrm{Re}_x{}^{-0.5} = -\Phi'(0).$$

3. Solution Methodology (HAM)

The optimal technique is used for the solution of the proposed model. The system of Equations (10),(11),(12) along with condition (18) is solved in Mathematica software via HAM. The method was first introduced by Liao [54, 55], and this method is frequently used in recent research [53, 56–62]. The HAM algorithm in Mathematica software is outlined as follows:

$$\widehat{F}(\eta) = 1 - e^{-\eta}, \widehat{\Theta}(\eta) = e^{-\eta}, \widehat{\Phi}(\eta) = e^{-\eta}, \tag{27}$$

Linear operators $L_{\widehat{F}}$, $L_{\widehat{\Theta}}$, and $L_{\widehat{\Phi}}$ are presumed as follows:$L_{\widehat{F}}(\widehat{F}) = \widehat{F}'''$, $\mathrm{L}_{\widehat{\Theta}}(\widehat{\Theta}) = \widehat{\Theta}''$, $\mathrm{L}_{\widehat{\Phi}}(\widehat{\Phi}) = \widehat{\Phi}''$.

$$L_{\widehat{F}}\left(\mathbb{N}_1 + \mathbb{N}_2\eta + \mathbb{N}_3\eta^2\right) = 0,$$
$$L_{\widehat{\Theta}}(\mathbb{N}_4 + \mathbb{N}_5\eta) = 0, \tag{28}$$
$$L_{\widehat{\Phi}}(\mathbb{N}_6 + \mathbb{N}_7\eta) = 0.$$

Here, we point out nonlinear terms that are specifically named as $N_{\widehat{F}}$, $N_{\widehat{\Theta}}$, and $N_{\widehat{\Phi}}$ in the algorithm:

$$N_{\widehat{F}}\left[\widehat{F}(\eta;\zeta)\right] = \widehat{F}_{\eta\eta\eta} + \left[\widehat{F}\widehat{F}_{\eta\eta} - \widehat{F}_{\eta\eta}^{2}\right] + \cos\theta\left[\mathrm{Gr}\widehat{\Theta} + \mathrm{Gr}^*\left(\widehat{\Theta}\right)^2 + \mathrm{Gc}\widehat{\Phi} + \mathrm{Gc}^*\left(\widehat{\Phi}\right)^2\right],$$
$$N_{\widehat{\Theta}}\left[\widehat{F}(\eta;\zeta), \widehat{\Theta}(\eta;\zeta)\right] = \widehat{\Theta}_{\eta\eta} + \mathrm{Pr}\widehat{F}\widehat{\Theta}_{\eta},$$
$$N_{\widehat{\Phi}}\left[\widehat{F}(\eta;\zeta), \widehat{\Phi}(\eta;\zeta)\right] = \widehat{\Phi}_{\eta\eta} + \mathrm{Sc}\widehat{F}\widehat{\Phi}_{\eta}. \tag{29}$$

For Equations (1),(2),(3), the zero-order system is

$$(1-\zeta)L_{\widehat{F}}\left[\widehat{F}(\eta;\zeta) - \widehat{F}_0(\eta)\right] = p\hbar_{\widehat{F}}N_{\widehat{F}}\left[\widehat{F}(\eta;\zeta)\right],$$
$$(1-\zeta)L_{\widehat{\Phi}}\left[\widehat{\Phi}(\eta;\zeta) - \widehat{\Phi}_0(\eta)\right] = p\hbar_{\widehat{\Phi}}N_{\widehat{\Phi}}\left[F(\eta;\zeta), \widehat{\Phi}(\eta;\zeta)\right],$$
$$(1-\zeta)L_{\widehat{\Theta}}\left[\widehat{\Theta}(\eta;\zeta) - \widehat{\Theta}_0(\eta)\right] = p\hbar_{\widehat{\Theta}}N_{\widehat{\Theta}}\left[F(\eta;\zeta), \widehat{\Theta}(\eta;\zeta)\right], \tag{30}$$

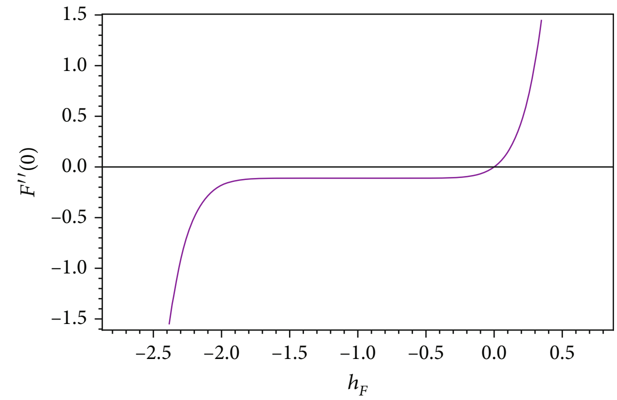

Figure 2: Velocity profile h curve.

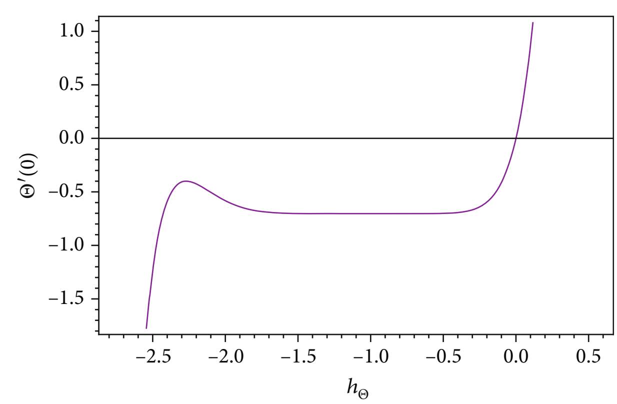

Figure 3: Temperature profile h curve.

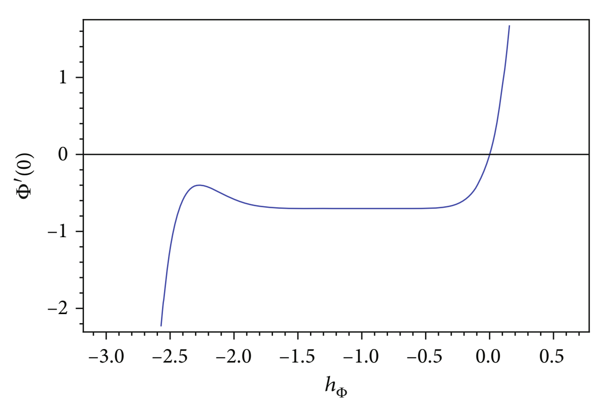

Figure 4: Concentration profile h curve.

while BCs are

$$\widehat{F}(\eta;\zeta)\Big|_{\eta=0} = 0, \frac{\partial\widehat{F}(\eta;\zeta)}{\partial\eta}\Big|_{\eta=0} = 1,$$
$$\widehat{\Theta}(\eta;\zeta)\Big|_{\eta=0} = 1, \widehat{\Phi}(\eta;\zeta)\Big|_{\eta=0} = 1,$$
$$\widehat{F}(\eta;\zeta)\Big|_{\eta=\infty} \longrightarrow 0, \widehat{\Theta}(\eta;\zeta)\Big|_{\eta=\infty} \longrightarrow 0, \widehat{\Phi}(\eta;\zeta)\Big|_{\eta=\infty} \longrightarrow 0. \tag{31}$$

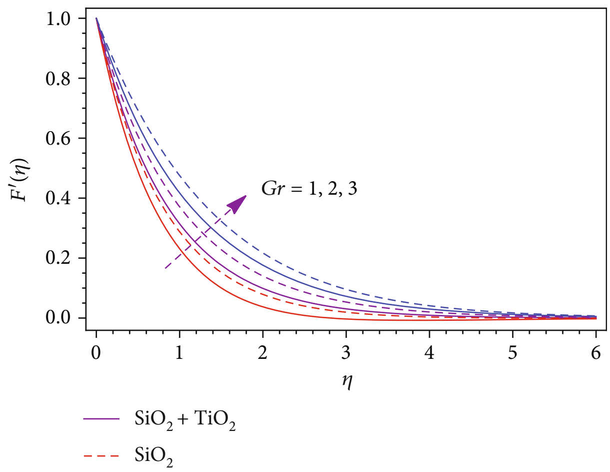

FIGURE 5: Effect of Grashof number on the velocity field.

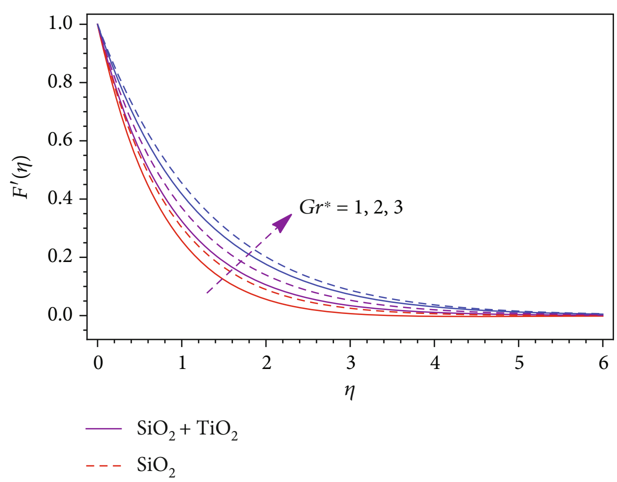

FIGURE 6: Impact of Grashof number (Gr^*) at the velocity field.

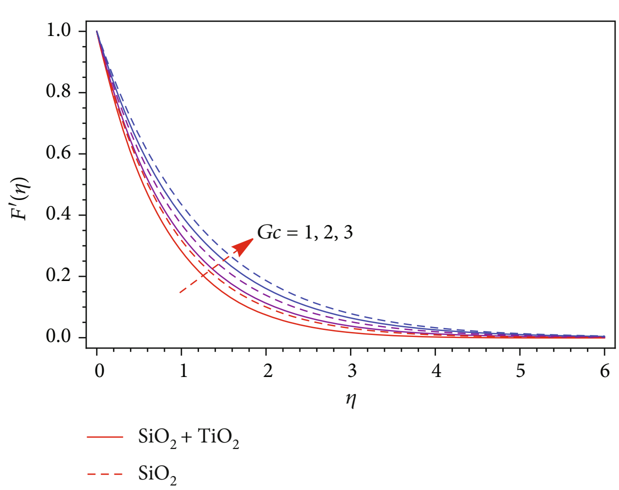

FIGURE 7: Impact of mass Grashof number (Gc) at the velocity field.

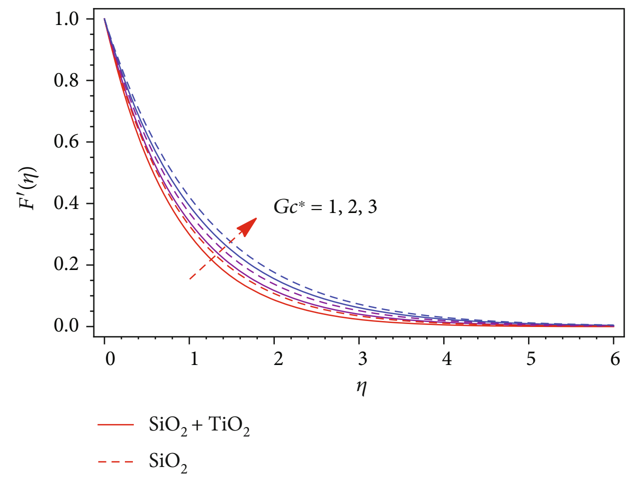

FIGURE 8: Effect of nonlinear mass Grashof number (Gc^*) on the velocity field.

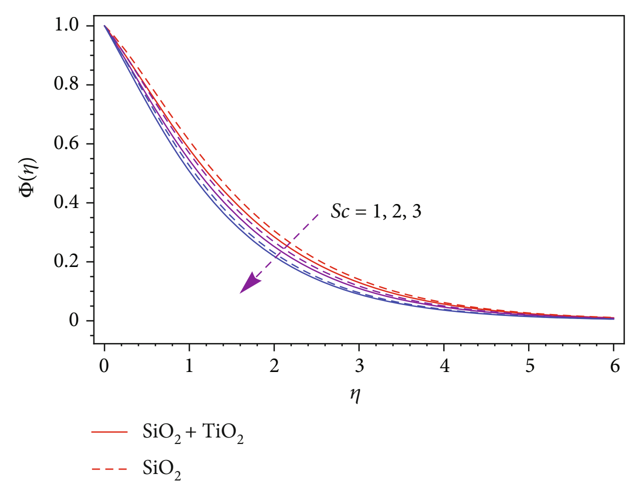

FIGURE 9: Influence of Schmidt number against concentration profile.

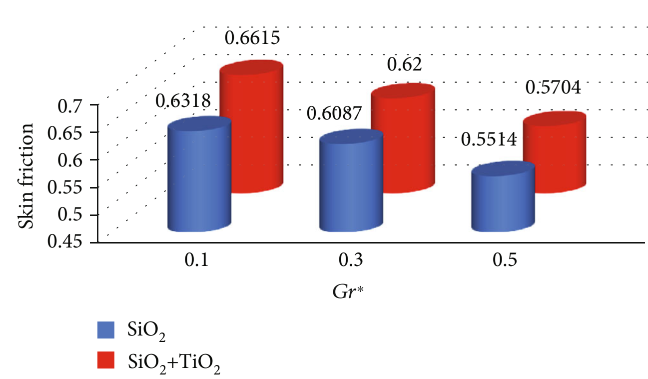

FIGURE 10: Skin friction versus thermal Grashof number.

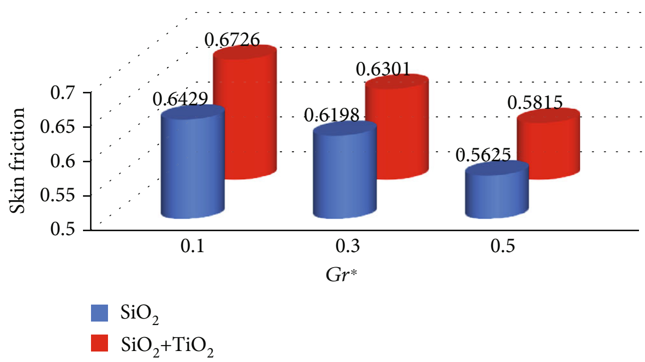

FIGURE 11: Skin friction versus nonlinear thermal Grashof number.

Now,

$$\mathfrak{R}_n^{\widehat{F}}(\eta) = \widehat{F'''}_{n-1} + \left[\sum_{j=0}^{w-1} \widehat{F}_{w-1-j}\widehat{F}''_j - \widehat{F'}^{\,2}_{n-1}\right] + \cos\theta\left[\sum_{j=0}^{w-1} \mathrm{Gr}\widehat{\Theta}_{w-1-j} + \mathrm{Gr}^*\left(\widehat{\Theta}_{n-1}\right)^2 + \sum_{j=0}^{w-1}\mathrm{Gc}\widehat{\Phi}_{n-1} + \sum_{j=0}^{w-1}\mathrm{Gc}^*\left(\widehat{\Phi}_{n-1}\right)^2\right] = 0,$$

$$\mathfrak{R}_n^{\widehat{\Theta}}(\eta) = \widehat{\Theta}''_{n-1} + \mathrm{Pr}\sum_{j=0}^{w-1}\widehat{F}_{w-1-j}\widehat{\Theta}'_j = 0,$$

$$\mathfrak{R}_n^{\widehat{\Phi}}(\eta) = \widehat{\Phi}''_{n-1} + \mathrm{Sc}\sum_{j=0}^{w-1}\widehat{F}_{w-1-j}\widehat{\Phi}'_j = 0, \tag{32}$$

while

$$\chi_n = \begin{cases} 0, & \text{if } \zeta \le 1, \\ 1, & \text{if } \zeta > 1. \end{cases} \tag{33}$$

3.1. Convergence of HAM Solution. The secondary conditions $\hbar_{\tilde{f}}, \hbar_{\tilde{\theta}}$, and$\hbar_{\tilde{\phi}}$ totally become a source for the convergence of Equations (5),(7),(9); this is why the series solution has been chosen for controlling and merging. The probability sector of $\hbar$ is generated different $\hbar$ curves of $\widetilde{f''}(0), \widetilde{\theta'}(0)$, and$\widetilde{\phi'}(0)$ in the approximated 20th order HAM-based solution using Mathematica. The effective region of $\hbar$ is $-1.5 < \hbar_{\tilde{f}} < 0.0, -1.5 < \hbar_{\tilde{\theta}} < 0.0$, and $-2.5 < \hbar_{\tilde{\phi}} < 0.0$. The convergence of HAM algorithm via $\hbar$ curves for the three important profiles like temperature, velocity, and concentration has been sketched in various graphs (2–4), correspondingly. Figure 2 is the h curve for the velocity profile, Figure 3 is the h curve for the temperature field, and Figure 4 is the h curve for the concentration profile.

Figure 5 explains the behaviour of the proposed flow model through the various values of Grashof number (Gr). The sketch reveals that an increment in the value of Gr augments the liquid velocity. The reality furthers is, since (Thermal Grashof Number) integrates both hydrodynamic forces and the thermal buoyancy force, which occurs in the boundary layer due to variation in temperature. Therefore, increasing the thermal buoyancy effect of the liquid permits the specified fluid to cool the hot plate.

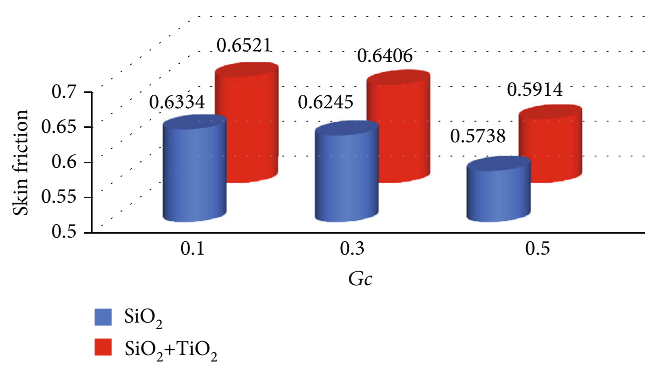

FIGURE 12: Skin friction versus mass Grashof number.

The impact of the Grashof number (Gr^*) which is caused by nonlinear convection enhances the movement of fluid relatively larger and more related to natural phenomena and shown in Figure 6.

Figure 7 explains the flow properties at various values of mass Grashof number (Gc). It reveals that a rise in the value of mass Grashof number increments the fluid velocity.

Figure 8 explains the flow properties at various values of mass Grashof number (Gc^*). It reveals that a rise in the value of mass Grashof of number (Gc^*) increments the velocity of the fluid.

The influence of Sc (Schmidt number) at the concentration profile is sketched in Figure 9, indicating that the enhancement of the value of Sc decrements the liquid concentration profile. The ratio of two properties such as momentum diffusion to mass diffusion is referred to as Sc. Therefore, for the larger value of Sc, the mass diffusion is due to momentum diffusion. While Sc increments, because of less mass diffusion and smaller D_B, the $\Phi(\eta)$ profile diminishes.

The thermal Grashof number and nonlinear thermal Grashof enhance the fluid motion and consequently decline the skin friction as shown in Figures 10 and 11.

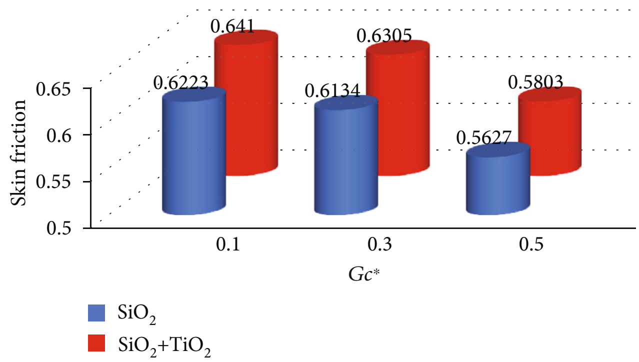

FIGURE 13: Skin friction versus nonlinear thermal Grashof number.

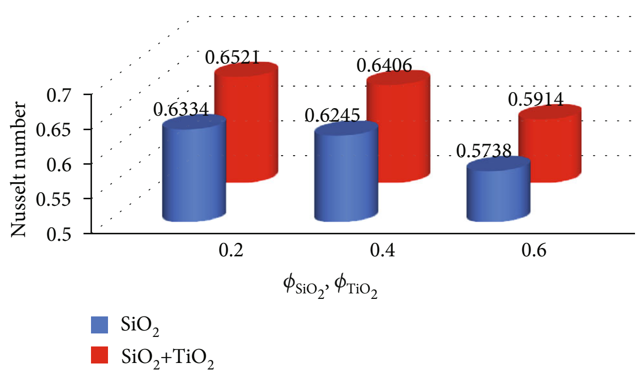

FIGURE 14: Heat transfer rate skin friction versus nanoparticle volume fraction.

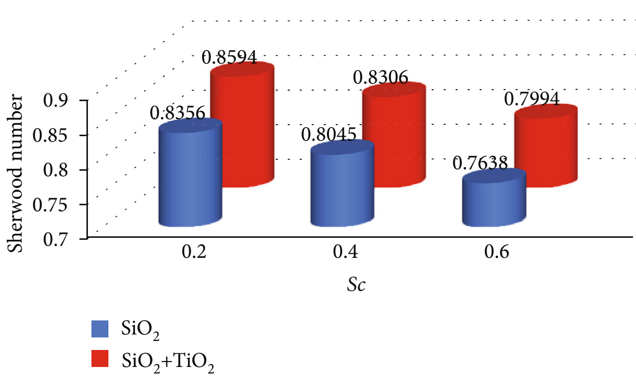

FIGURE 15: Mass transfer rate versus Schmidt number.

Furthermore, the effect is comparatively more impressible using the hybrid nanofluid.

The mass Grashof number and nonlinear mass Grashof strengthen the fluid velocity and consequently decline the skin friction as shown in Figures 12 and 13. Furthermore, the effect is comparatively more impressible using the hybrid nanofluid.

The hybrid nanofluids have the tendency to improve the thermal efficiency as shown in Figure 14. The heat transfer rate is comparatively more effective using the hybrid nanofluids. Physically, the thermal combined thermal conductivity of these nanoparticles is more reliable for the enhancement of heat transfer.

TABLE 1: Comparison of the present work with published work [63] considering $-(k_{\eta f}/k_f)\Theta'(0)$.

	$-(k_{\eta f}/k_f)\Theta'(0)$ [65]	$\mathrm{Pr} - (k_{\eta f}/k_f)\Theta'(0)$ Present
6	0.789320421	0.789331322
7	0.77842876231	0.7784421573
8	0.76776543212	0.7677432641

The mass transfer declines with the increasing amount of Sc as shown in Figure 15. The Schmidt number also declines the concentration for its increasing values; that is why the mass transfer also declines.

The present work is compared with the published work [60] as shown in Table 1 by considering the common parameters. It is concluded that the obtained results closely agreed with the published work.

4. Conclusion

In the present section, we evaluated the nonlinear convective fluid flow over an inclined plane considering heat and mass transfer analysis. The nonlinear convection is mainly focused to study the flow field down the inclined plane.

The highlights of the current work are as follows:

(i) The nonlinear convection provides two Grashof numbers that represent linear and nonlinear phenomena. The greater values of both the thermal Grashof numbers increase the fluid motion for its larger values

(ii) The mass Grashof numbers also used nonlinear and are more relevant to the natural phenomena. The increasing values of these parameters improve the fluid motion

(iii) The obtained results illustrate that hybrid nanofluids are more affective for the heat transfer analysis

(iv) The concentration field reduces with the greater value of Sc

Data Availability

All the relevant data exist in the manuscript.

Conflicts of Interest

The authors declare that no such interest exists.

Acknowledgments

The authors extend their appreciation to the Deanship of Scientific Research at King Khalid University for funding this work through research groups under grant number R.G.P.2/14/43.

References

[1] N. Sandeep and A. Malvandi, "Enhanced heat transfer in liquid thin film flow of non-Newtonian nanofluids embedded with graphene nanoparticles," *Advanced Powder Technology.*, vol. 27, no. 6, pp. 2448–2456, 2016.

[2] C. Y. Wang, "Liquid film on an unsteady stretching surface," *Quarterly of Applied Mathematics*, vol. 48, no. 4, pp. 601–610, 1990.

[3] R. Usha and R. Sridharan, "On the motion of a liquid film on an unsteady stretching surface," *ASME Fluids Engineering*, vol. 150, pp. 43–48, 1993.

[4] I. C. Liu and H. I. Andersson, "Heat transfer in a liquid film on an unsteady stretching sheet," *International Journal of Thermal Sciences*, vol. 47, no. 6, pp. 766–772, 2008.

[5] R. C. Aziz, I. Hashim, and A. K. Alomari, "Thin film flow and heat transfer on an unsteady stretching sheet with internal heating," *Meccanica*, vol. 46, no. 2, pp. 349–357, 2011.

[6] L. Tawade and M. Abel, "Thin film flow and heat transfer over an unsteady stretching sheet with thermal radiation, internal heating in presence of external magnetic field," *International journal of advances in applied mathematics and mechanics*, vol. 3, pp. 29–40, 2016.

[7] H. I. Anderssona, J. B. Aarseth, and B. S. Dandapatb, "Heat transfer in a liquid film on an unsteady stretching surface," *International Journal of Heat and Mass Transfer*, vol. 43, no. 1, pp. 69–74, 2000.

[8] C. H. Chen, "Heat transfer in a power-law fluid film over a unsteady stretching sheet," *Heat and Mass Transfer.*, vol. 39, no. 8-9, pp. 791–796, 2003.

[9] C. H. Chen, "Effect of viscous dissipation on heat transfer in a non-Newtonian liquid film over an unsteady stretching sheet," *Journal of Non-Newtonian Fluid Mechanics*, vol. 135, no. 2-3, pp. 128–135, 2006.

[10] C. Wang and L. Pop, "Analysis of the flow of a power-law fluid film on an unsteady stretching surface by means of homotopy analysis method," *Journal of Non-Newtonian Fluid Mechanics*, vol. 138, no. 2-3, pp. 161–172, 2006.

[11] M. A. Mahmoud, "On flow and heat transfer in a thin liquid film over an unsteady stretching sheet with variable fluid properties and radiation," *Open Science journal of Mathematics and Application*, vol. 3, no. 1, pp. 14–18, 2015.

[12] A. M. Megahe, "Effect of slip velocity on Casson thin film flow and heat transfer due to unsteady stretching sheet in presence of variable heat flux and viscous dissipation," *Applied Mathematics and Mechanics*, vol. 36, no. 10, pp. 1273–1284, 2015.

[13] F. Tahir, T. Gul, S. Islam et al., "Flow of a nano-liquid film of Maxwell fluid with thermal radiation and magneto hydrodynamic properties on an unstable stretching sheet," *Journal of Nanofluids*, vol. 6, pp. 1–10, 2017.

[14] N. S. Khan, T. Gul, S. Islam, A. Kha, and Z. Shah, "Brownian motion and thermophoresis effects on MHD mixed convective thin film second-grade nanofluid flow with Hall effect and heat transfer past a stretching sheet," *Journal of Nanofluids*, vol. 6, no. 5, pp. 812–829, 2017.

[15] O. Rejeb, M. S. Yousef, C. Ghenai, H. Hassan, and M. Bettaye, "Investigation of a solar still behaviour using response surface methodology," *Case Studies in Thermal Engineering*, vol. 24, p. 100816, 2021.

[16] U. S. Choi, "Enhancing thermal conductivity of fluids with nanoparticles," *AS-MEFED*, vol. 231, pp. 99–103, 1995.

[17] K. Khanafer and K. Vafai, "A review on the applications of nanofluids in solar energy field," *Renewable Energy*, vol. 123, pp. 398–406, 2018.

[18] H. T. Basha, R. Sivaraj, A. S. Reddy, and A. Chamkha, "SWCNH/diamond ethylene glycol nanofluid flow over a wedge, plate and stagnation point with induced magnetic field and nonlinear radiation-solar energy application," *The European Physical Journal Special Topics*, vol. 228, no. 12, pp. 2531–2551, 2019.

[19] A. Izadi, M. Siavashi, and Q. Xiong, "Impingement jet hydrogen, air and CuH2O nanofluid cooling of a hot surface covered by porous media with non-uniform input jet velocity," *International Journal of Hydrogen Energy*, vol. 44, no. 30, pp. 15933–15948, 2019.

[20] M. Siavashi and S. M. M. Joibary, "Numerical performance analysis of a counter-flow double-pipe heat exchanger with using nanofluid and both sides partly filled with porous media," *Journal of Thermal Analysis and Calorimetry*, vol. 135, no. 2, pp. 1595–1610, 2019.

[21] F. Mebarek-Oudina, "Convective heat transfer of Titania nanofluids of different base fluids in cylindrical annulus with discrete heat source," *Heat Transfer—Asian Research*, vol. 48, no. 1, pp. 135–147, 2019.

[22] A. Saeed and T. Gul, "Bioconvection Casson nanofluid flow together with Darcy-Forchheimer due to a rotating disk with thermal radiation and Arrhenius activation energy," *SN Applied Sciences*, vol. 3, no. 1, pp. 1–19, 2021.

[23] S. Rehman, T. Gul, W. Khan, A. Khan, and Zeeshan, "Effects of chemical reaction, viscosity, thermal conductivity, heat source, radiation/absorption, on MHD mixed convection nano-fluids flow over an unsteady stretching sheet by HAM and numerical method," *Advances in Mechanical Engineering*, vol. 14, no. 1, 2022.

[24] R. Sajjad, T. Hayat, R. Ellahi, T. Muhammad, and A. Alsaedi, "Darcy–Forchheimer flow of nanofluid due to a curved stretching surface," *International Journal of Numerical Methods for Heat & Fluid Flow*, vol. 29, no. 1, pp. 2–20, 2019.

[25] M. Sheikholeslami, "Magnetic field influence on CuO-H_2O nanofluid convective flow in a permeable cavity considering various shapes for nanoparticles," *International Journal of Hydrogen Energy*, vol. 42, no. 31, pp. 19611–19621, 2017.

[26] L. Zhang, M. M. Bhatti, R. Ellahi, and E. M. Efstathios, "Oxytactic microorganism and thermo-bioconvection nanofluid flow over a porous Riga plate having Darcy-Brinkman-Forchheimer medium," *Journal of Non-Equilibrium Thermodynamics*, vol. 5, no. 3, pp. 257–268, 2020.

[27] T. Gul, S. Nasir, S. Islam, Z. Shah, and M. A. Khan, "Effective Prandtl number model influences on the γAl_2O_3-H_2O and γAl_2O_3-$C_2H_6O_2$ nanofluids spray along a stretching cylinder," *Arabian Journal for Science & Engineering*, vol. 44, no. 2, pp. 1–22, 2019.

[28] H. Alfvén, "Existence of electromagnetohydrodynamic waves," *Nature*, vol. 150, no. 3805, pp. 405-406, 1942.

[29] W. D. Jackson, J. H. Olsen, and A. T. Lewis, *Plasma magnetohydrodynamics and energy conversion*, Research Laboratory of Electronics (RLE) at the Massachusetts Institute of Technology (MIT), 1963.

[30] M. M. Rashidi, S. Abelman, and N. F. Mehr, "Entropy generation in steady MHD flow due to a rotating porous disk in a nanofluid," *International Journal of Heat and Mass Transfer*, vol. 62, pp. 515–525, 2013.

[31] W. A. Khan and I. Pop, "Boundary-layer flow of a nanofluid past a stretching sheet," *International Journal of Heat and Mass Transfer*, vol. 53, no. 11-12, pp. 2477–2483, 2010.

[32] M. M. Rashidi and E. Erfani, "The modified differential transform method for investigating nano boundary-layers over stretching surfaces," *International Journal of Numerical Methods for Heat & Fluid Flow*, vol. 21, no. 7, pp. 864–883, 2011.

[33] Z. Abdel-Nour, A. Aissa, F. Mebarek-Oudina et al., "Magnetohydrodynamic natural convection of hybrid nanofluid in a porous enclosure: numerical analysis of the entropy generation," *Journal of Thermal Analysis and Calorimetry*, vol. 141, no. 5, pp. 1981–1992, 2020.

[34] F. Mebarek-Oudina and R. Bessaih, "Oscillatory magnetohydrodynamic natural convection of liquid metal between vertical coaxial cylinders," *Journal of Applied Fluid Mechanics*, vol. 9, no. 6, pp. 1655–1665, 2016.

[35] F. Mebarek-Oudina, A. Aissa, B. Mahanthesh, and H. F. Öztop, "Heat transport of magnetized Newtonian nanoliquids in an annular space between porous vertical cylinders with discrete heat source," *International Communications in Heat and Mass Transfer*, vol. 117, p. 104737, 2020.

[36] P. Forchheimer, "Wasserbewegung durch boden," *Zeitschrift des Vereins Deutscher Ingenieure*, vol. 45, pp. 1782–1788, 1901.

[37] M. Muskat, *The Flow of Homogeneous Fluids through Porous Media*, McGraw-Hill, New York, 1946.

[38] G. Rasool, A. Shafiq, C. M. Khalique, and T. Zhang, "Magnetohydrodynamic Darcy-Forchheimer nanofluid flow over a nonlinear stretching sheet," *Physica Scripta*, vol. 94, no. 10, article 105221, 2019.

[39] M. A. Sadiq, F. Haider, T. Hayat, and A. Alsaedi, "Partial slip in Darcy-Forchheimer carbon nanotubes flow by rotating disk," *International Communications in Heat and Mass Transfer*, vol. 116, p. 104641, 2020.

[40] M. Sheikholeslami, A. Arabkoohsar, and K. A. R. Ismail, "Entropy analysis for a nanofluid within a porous media with magnetic force impact using non-Darcy model," *International Communications in Heat and Mass Transfer*, vol. 112, p. 104488, 2020.

[41] T. Hayat, S. A. Khan, A. Alsaedi, and H. M. Fardoun, "Heat transportation in electro-magnetohydrodynamic flow of Darcy-Forchheimer viscous fluid with irreversibility analysis," *Physica Scripta*, vol. 95, no. 10, p. 105214, 2020.

[42] T. Hayat, F. Haider, and A. Alsaedi, "Darcy-Forchheimer flow with nonlinear mixed convection," *Applied Mathematics and Mechanics*, vol. 41, no. 11, pp. 1685–1696, 2020.

[43] K. G. Kumar, M. Rahimi-Gorji, M. G. Reddy, A. J. Chamkha, and I. M. Alarifi, "Enhancement of heat transfer in a convergent/divergent channel by using carbon nanotubes in the presence of a Darcy–Forchheimer medium," *Microsystem Technologies*, vol. 26, no. 2, pp. 323–332, 2020.

[44] M. Partohaghighi, E. Karatas Akgül, G. W. Weber, G. Yao, and A. Akgül, "Recovering source term of the time-fractional diffusion equation," *Pramana*, vol. 95, no. 4, pp. 1–8, 2021.

[45] A. Akgül, "A novel method for a fractional derivative with non-local and non-singular kernel," *Chaos, Solitons & Fractals*, vol. 114, pp. 478–482, 2018.

[46] E. K. Akgül, A. Akgül, and M. Yavuz, "New illustrative applications of integral transforms to financial models with different fractional derivatives," *Chaos, Solitons & Fractals*, vol. 146, p. 110877, 2021.

[47] E. Karatas Akgül, A. Akgül, and D. Baleanu, "Laplace transform method for economic models with constant proportional Caputo derivative," *Fractal and Fractional*, vol. 4, no. 3, p. 30, 2020.

[48] S. Bilal, I. A. Shah, A. Akgül et al., "Finite difference simulations for magnetically effected swirling flow of Newtonian liquid induced by porous disk with inclusion of thermophoretic particles diffusion," *Alexandria Engineering Journal*, vol. 61, no. 6, pp. 4341–4358, 2022.

[49] N. A. Shah, S. Saleem, A. Akgül, K. Nonlaopon, and J. D. Chung, "Numerical analysis of time-fractional diffusion equations via a novel approach," *Journal of Function Spaces*, vol. 2021, Article ID 9945364, 12 pages, 2021.

[50] A. Dawar, E. Bonyah, S. Islam, A. Alshehri, and Z. Shah, "Theoretical analysis of Cu-H_2O, Al_2O_3-H_2O, and TiO_2-H_2O nanofluid flow past a rotating disk with velocity slip and convective conditions," *Journal of Nanomaterials*, vol. 2021, Article ID 5471813, 10 pages, 2021.

[51] M. Z. Ullah, D. Abuzaid, M. Asma, and A. Bariq, "Couple stress hybrid nanofluid flow through a converging-diverging channel," *Journal of Nanomaterials*, vol. 2021, Article ID 2355258, 13 pages, 2021.

[52] T. S. Khan, N. Sene, A. Mouldi, and A. Brahmia, "Heat and mass transfer of the Darcy-Forchheimer Casson hybrid nanofluid flow due to an extending curved surface," *Journal of Nanomaterials*, vol. 2022, 2022.

[53] M. Jawad, A. Saeed, T. Gul, Z. Shah, and P. Kumam, "Unsteady thermal Maxwell power law nanofluid flow subject to forced thermal Marangoni convection," *Scientific Reports*, vol. 11, no. 1, pp. 1–14, 2021.

[54] S. J. Liao, "An optimal homotopy-analysis approach for strongly nonlinear differential equations," *Communications in Nonlinear Science and Numerical Simulation*, vol. 15, no. 8, pp. 2003–2016, 2010.

[55] S. J. Liao, Ed., *Advances in the Homotopy Analysis Method, chapter7*, World Scientific Press, 2014.

[56] T. Gul and K. Ferdous, "The experimental study to examine the stable dispersion of the graphene nanoparticles and to look at the GO–H2O nanofluid flow between two rotating disks," *Nano*, vol. 8, no. 7, pp. 1711–1727, 2018.

[57] M. Jawad, A. Saeed, T. Gul, and A. Bariq, "MHD Darcy-Forchheimer flow of Casson nanofluid due to a rotating disk with thermal radiation and Arrhenius activation energy," *Journal of Physics Communications.*, vol. 5, no. 2, article 025008, 2021.

[58] A. Rehman, Z. Salleh, and T. Gul, "Heat transfer of thin film flow over an unsteady stretching sheet with dynamic viscosity," *Journal of Advanced Research in Fluid Mechanics and Thermal Sciences*, vol. 81, no. 2, pp. 67–81, 2021.

[59] A. Khan, W. Kumam, I. Khan et al., "Chemically reactive nanofluid flow past a thin moving needle with viscous dissipation, magnetic effects and hall current," *PLoS One*, vol. 16, no. 4, p. e0249264, 2021.

[60] A. Khan, A. Saeed, A. Tassaddiq et al., "Bio-convective micropolar nanofluid flow over thin moving needle subject to Arrhenius activation energy, viscous dissipation and binary chemical reaction," *Case Studies in Thermal Engineering*, vol. 25, p. 100989, 2021.

[61] M. Bilal, A. A. Gul, A. Alsubie, and I. Ali, "Axisymmetric hybrid nanofluid flow with heat and mass transfer amongst the two gyrating plates," *Zeitschrift für Angewandte Mathematik und Mechanik*, vol. 101, no. 11, 2021.

[62] L. Ali, A. Tassaddiq, R. Ali et al., "A new analytical approach for the research of thin-film flow of magneto hydrodynamic fluid in the presence of thermal conductivity and variable viscosity," *ZAMM-Journal of Applied Mathematics and Mechanics/Zeitschrift für Angewandte Mathematik und Mechanik*, vol. 101, no. 2, 2021.

[63] A. K. Alzahrani, M. Z. Ullah, A. S. Alshomrani, and T. Gul, "Hybrid nanofluid flow in a Darcy-Forchheimer permeable medium over a flat plate due to solar radiation," *Case Studies in Thermal Engineering*, vol. 26, p. 100955, 2021.